Proceedings of The Canadian Society for Mechanical Engineering International Congress 2016
CSME International Congress 2016
June 26-29, 2016, Kelowna, BC, Canada

Optimal inter-area transfer in the presence of demand response and renewable electricity generation

Sahand Behboodi, Curran Crawford, Ned Djilali
Department of Mechanical Engineering and Institute for Integrated Energy Systems, University of Victoria
Victoria, Canada
Behboodi@uvic.ca, curranc@uvic.ca
ndjilali@uvic.ca

David P. Chassin
Department of Mechanical Engineering and Institute for Integrated Energy Systems, University of Victoria, and Pacific Northwest National Laboratory
Richland, Washington, USA
david.chassin@pnnl.gov

Abstract— This paper describes the impact of demand response and intermittent renewable resources integration on electricity generation and inter-change scheduling. A surplus maximizing method is proposed and tested on a hypothetical system of two consolidated areas that loosely represent the North America's Western Interconnection (separated by the Canada-United States border). An hourly electricity market is assigned to each area, and the power exchange that achieves the maximum surplus is obtained for the planning year of 2024. The solution is then modified to account for the existing path transfer capacity, 3150 MW North-South and 3000 MW South-North. The path economic utilization factor, the ratio of the surplus increase to the maximum surplus increase, is 31%. The economic power transfer distribution factor, the metric used to quantify the sensitivity of the power flow with respect to the price difference, is 67 MW/($/MWh). In addition, the optimal schedule is sought for cases when path transfer capacity is expanded by 1000 MW and 2000 MW. The same study is performed for year 2030, assuming the additional wind electricity meets the demand growth. Results show the economic utilization factor increases to 32%, and the economic power transfer distribution factor increases to 84 MW/($/MWh).

Keywords: Demand response; variable generation; scheduling; surplus; electricity market; tie-line transfer capacity

I. INTRODUCTION

Growing participation of renewable resources in the overall generation fleet has increased pressure on generators responsible for ensuring reliability to provide resources that mitigate renewable intermittency, without increasing overall GHG emissions. Demand response is widely regarded as a potentially significant class of zero-carbon reliability resources that can displace carbon-intensive reliability resources, such as natural gas combustion turbines and/or energy constrained reliability resources such as hydro-electric generators. The US Department of Energy has adopted a definition of demand response that is now widely recognized for its inclusiveness [1]: load variations in response to change in both financial incentives and/or reliability signals over time. The interaction between demand response and renewable resources in electricity markets is a well-studied topic [2-7].

Given an inelastic demand, the market finds the generation and inter-change schedules that minimizes the operational costs; however, in the presence of demand response, the market finds the schedule that maximizes the total surplus [8]. Total surplus is defined as consumer monetary value minus producer cost [9]. We present a methodology to investigate the impact of demand response implementation on generation and inter-change scheduling. The proposed method is tested on a hypothetical system consisting of two areas that loosely represent the North America's Western Interconnection, known as the Western Electricity Coordinating Council (WECC), including 14 Western States, two Canadian Provinces and Baja California in Mexico. Area 1 is the consolidation of British Columbia and Alberta power grids, and Area 2 is the rest of the system.

In interconnected systems, transmission tie-lines enable balancing authorities to exchange electricity and share operating reserves. In the WECC system, balancing authorities exchange electricity to reduce their operational costs, although the interconnection is not operated according to a true optimal schedule, because of local regulations. As the penetration of variable generation resources increases, balancing authorities can collaborate more effectively to benefit from the geographical diversity of renewable resources in the interconnection, which requires an enhanced transmission system. Previous work [10] has shown potential savings in production cost due to consolidation of balancing authorities, with 8% wind and 3% solar energy penetration, ranges from 2.4% to 3.2% of the total yearly production cost, considering transmission congestion; the full copper-sheet consolidation of WECC shows an additional 1.4% improvement. A recent study [11] showed that the deployment of wind and solar power can reduce CO_2 emissions in the US by up to 80% relative to 1990 levels, without an increase in electricity price, by moving away

from a regionally divided electricity sector to a national system enabled by high-voltage direct-current transmission lines.

The inter-area exchange schedule is usually updated on an hourly basis; however, intra-hour scheduling should perhaps be used, since it has substantial cost benefits, particularly for cases with high penetrations of variable generation. A 10-minute exchange schedule has been shown to reduce the WECC production cost by 4% and 6% for intermittent renewable penetrations of 11% and 33%, respectively [12].

This paper examines the impact of demand response integration and transmission expansion on generation and inter-change schedules in the presence of variable generation resources, for WECC year 2024 and 2030 case studies. In Section II, a detailed description on the proposed scheduling method is provided. In Section III, optimal flow is determined for given assumptions, and the surplus increase is studied.

II. METHODOLOGY

A. Market Basics

The demand curve consists of a flat segment, including price-unresponsive loads, and a sloping segment including responsive loads. An approximation for the demand function is [13]:

$$Q_L(P) = \frac{Q_R}{1+e^{2\eta\left(1-\frac{P}{\bar{P}}\right)}} + Q_U, \qquad (1)$$

where Q_R is the maximum responsive demand, Q_U is the unresponsive load, η is the short-term price elasticity of demand, P is the dispatch price, and $\bar{P}$ is the average price. At equilibrium the responsive portion of demand has a symmetric shape, with an inflection point at $(Q_U + 0.5\,Q_R\,, \bar{P})$. The supply curve consists of a flat segment including must-run (usually zero-marginal cost) units and another sloping segment including non-zero bid units, which together form the "hockey stick" shape supply curve. An approximation for the supply function is [13]:

$$P(Q_G, Q_N) = c_1\left(1 - \frac{Q_G - Q_N}{Q_{max}}\right)^{-c_2} + c_3, \qquad (2)$$

where c_1, c_2 and c_3 are supply curve constants determined by the generation mixture, Q_{max} is the control area's maximum possible load with reserve requirements, and Q_N is non-dispatchable (must-run) generation. Fig. 1 shows the clearing condition. The intersection of these curves (equilibrium point) is the stand-alone clearing condition (Q_S, P_S). The blue and red hatched areas are the consumer and producer surpluses respectively.

Fig. 2 illustrates the impact of electricity export on the surplus. As the exports increase, the local consumption (Q_L) and consumer surplus decrease, while local production (Q_G) and producer surplus increase, as a result of the new higher clearing price (P_C). The total surplus increase is the solid red area. Similarly, for the importing jurisdiction, the production and producer surpluses decrease, while the local consumption, consumer and total surpluses increase. The producer surplus is obtained as:

$$\frac{P_C - c_3}{c_2 - 1} c_2\, Q_G - \frac{P_C - c_2\, c_3}{c_2 - 1} Q_N - \frac{P_C - c_1 - c_3}{c_2 - 1} Q_{max}. \qquad (3)$$

The consumer surplus for the elastic demands is:

$$(P_{max} - P_C)(Q_U + Q_R) - \frac{Q_R \bar{P}}{2\eta} \ln \frac{e^{2\eta\left(1-\frac{P_C}{\bar{P}}\right)}+1}{e^{2\eta\left(1-\frac{P_{max}}{\bar{P}}\right)}+1}, \qquad (4)$$

and for the inelastic demands is:

$$(P_{max} - P_C) Q_L. \qquad (5)$$

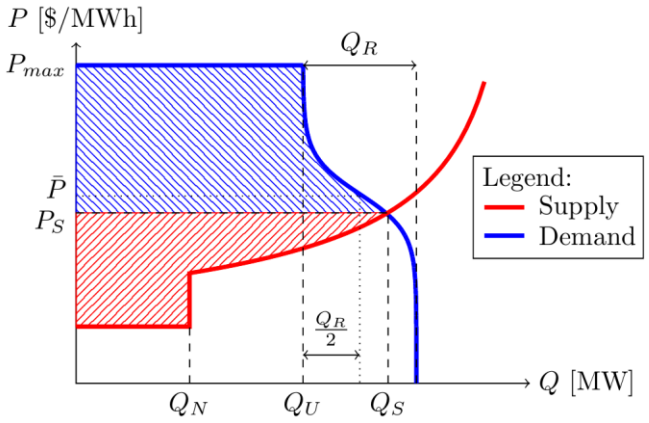

Figure 1. Market clearing process.

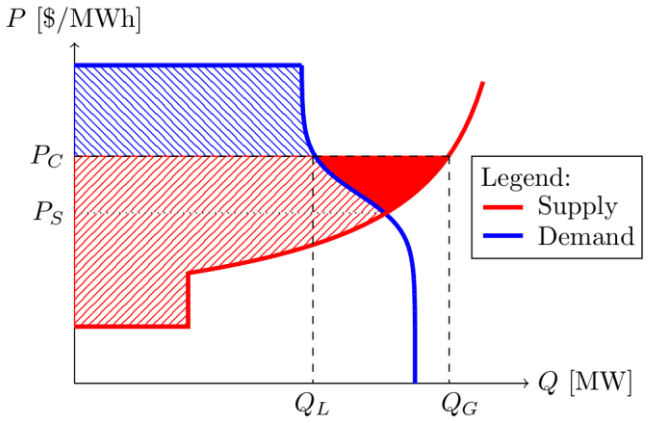

Figure 2. The impact of electricity export on surplus.

B. Problem Description

The purpose of interconnection scheduler is to establish inter-area flows such that the system (global) surplus increases, while considering system constraints. In every area the surplus includes the stand-alone surplus, which is invariant with respect to inter-area flows, and the additional inter-change surplus, which is variable. The scheduler maximizes the summation of additional surplus over the entire interconnected system's areas:

$$\max_f \sum_{m=1}^{M} interchange\ surplus_m, \qquad (6)$$

where f are the tie-line flows. The maximum surplus condition is achieved when the clearing price is uniform in the entire interconnection. However, there may be no flow solution that satisfies the ideal exports/imports within tie-line flow constraints. In this case, we seek the tie-line flow that increases

the surplus as much as possible given the constraints. The ratio of the additional surplus to the maximum additional surplus is a metric that defines the transmission system performance, which we refer to as the economic utilization factor (EUF). Accordingly, the path EUF is zero for stand-alone (no exchange) condition, and is 100% for the "copper-sheet" (unconstrained flow) condition.

Determination of the optimal flow is straightforward for a two-area system, because only one path exists. In hours that the optimal flow is beyond the path limit, the constraint is active, thus the actual flow should be truncated to the path transfer capacity, and the quantities and prices should be updated accordingly. Another performance metric, the economic power transfer distribution factor (EPTDF), is defined to quantify the sensitivity of flow with respect to price difference:

$$EPTDF = \frac{1}{8760}\sum_{t=1}^{8760}\left(\frac{f_{1\to 2}}{P_{s2}-P_{s1}}\right)_t, \qquad (7)$$

where P_{s1} and P_{s2} are stand-alone prices at hour t in Area 1 and Area 2, respectively.

The proposed method is summarized in the following steps. First, the stand-alone (the minimum global surplus), copper-sheet (the maximum global surplus) and constrained-flow solutions are obtained, assuming the load is completely inelastic, for given hourly demand and must-run generation profiles. Notice that the non-flat segment of the supply curve is assumed fixed for the whole study year. The opportunity price, defined as the next hour price for any hour, is found. Second, the demand curve is stated based on the logistic function given in (1), with an inflection point at the mean value of the hour price and the opportunity price, and a demand elasticity of -1. Third, the market clearing process is repeated with the elastic demand, and stand-alone demand and price are obtained. Next, the inter-change schedule that equalizes the prices is determined, and the annual maximum surplus increase is computed. At the end, the exchange is adjusted according to the path transfer capacity, and the actual surplus increase, the path EUF and EPTDF are computed.

C. Model inputs

An important assumption here is that each area has a uniform price, with no binding internal constraints that would result in different price zones within the area. This is not always a valid assumption for peak hours, but is easily remedied by increasing the number of areas defined in the model. The model inputs are taken from the WECC 2024 common case [15]. Fig. 3 shows the forecasted hourly load duration curve for the WECC 2024 model. We aggregate the intermittent renewable electricity (wind, solar and run-of-river hydro) in each area, to find the must-run generation. These resources have zero-marginal cost. Table I shows the capacity and capacity factor of wind electricity in Area 1 (Canada) and Area 2 (United States), taken from [15].

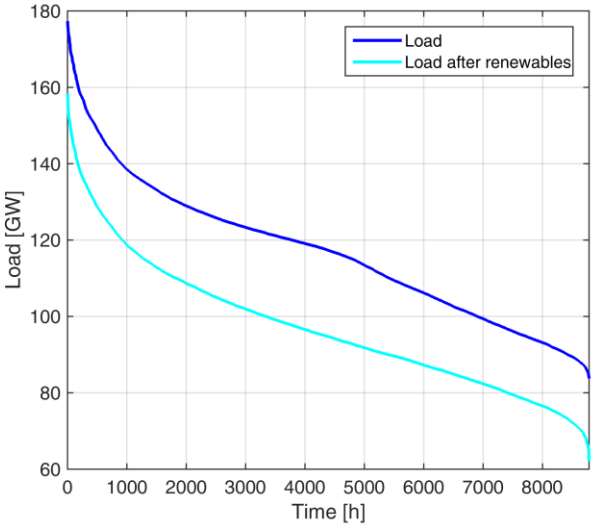

Figure 3. WECC load ducation curve.

TABLE I. WIND CHARACTERISTICS

Type	Area 1	Area 2
Capacity [MW]	3234	25918
Capacity factor [%]	33.26	28.53
Correlation coefficient	0.27	

Supply curve constants for a typical curve are taken from [14] as $c_1 = 4$ \$/MWh, $c_2 = 2.6$ and $c_3 = 11$ \$/MWh, and the market price cap is 1000 \$/MWh. Regarding the demand curve, we assume that the responsive portion of demand will be 10% if the cleared price is the same as the average price. In extremes, the magnitude of responsive demand will be: twice as the average price case if the price is zero; and zero if the price is at its cap.

III. RESULTS AND DISCUSSION

In this section, the simulation results for year 2024 and 2030 are provided. Demand response implementation moderates the price, as is clearly shown in Figs. 4 and 5.

Figs. 6 and 7 show both unconstrained and constrained flow versus the difference between stand-alone prices under the inelastic and elastic loads. The positive direction of path flow is from Area 1 to Area 2. The price difference is the stand-alone price in Area 2 minus the stand-alone price in Area 1. The unconstrained-flow EPTDF is 80 MW/(\$/MWh), and constrained-flow is 40 MW/(\$/MWh) for the inelastic load. Similarly, the unconstrained-flow EPTDF is 151 MW/(\$/MWh) and constrained-flow is 67 MW/(\$/MWh) for the elastic load. The price difference causes a relatively greater demand in the expensive side of the path, and a smaller demand in the cheap side of the path; therefore, increasing the path flow.

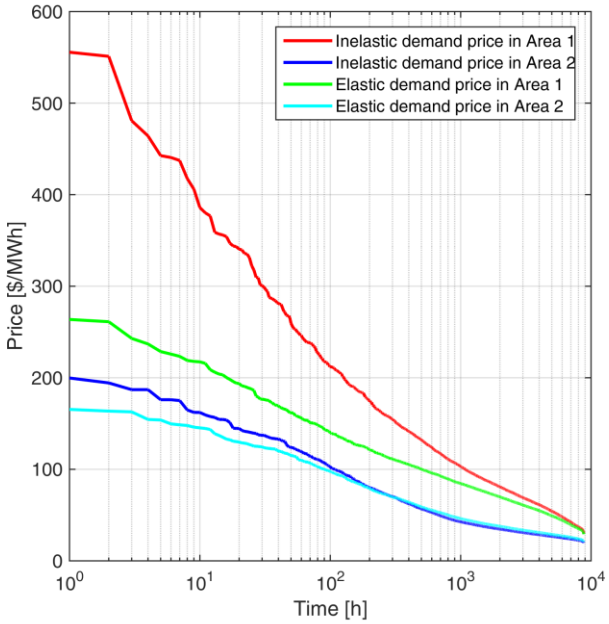

Figure 4. Price duration curve (stand-alone) year 2024.

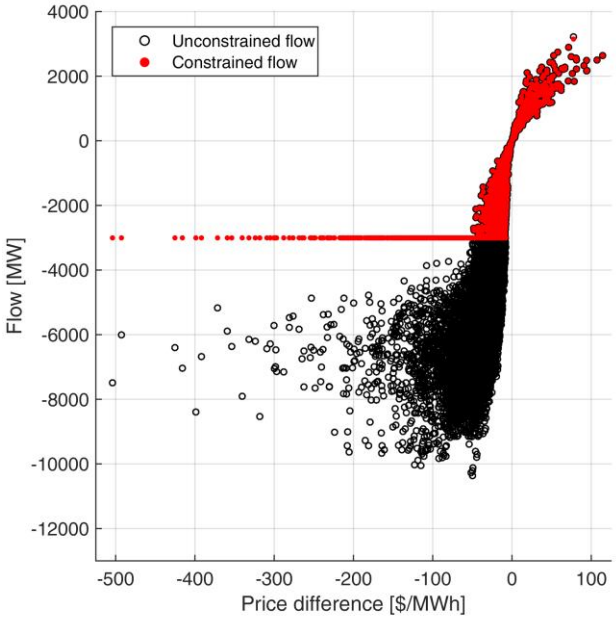

Figure 6. Flow sensitivity to the price difference (inelastic load) year 2024.

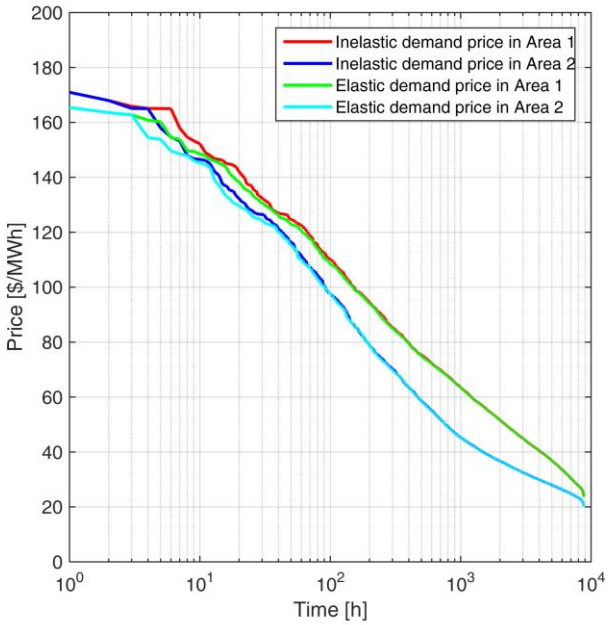

Figure 5. Price duration curve (with transfer constraint) year 2024.

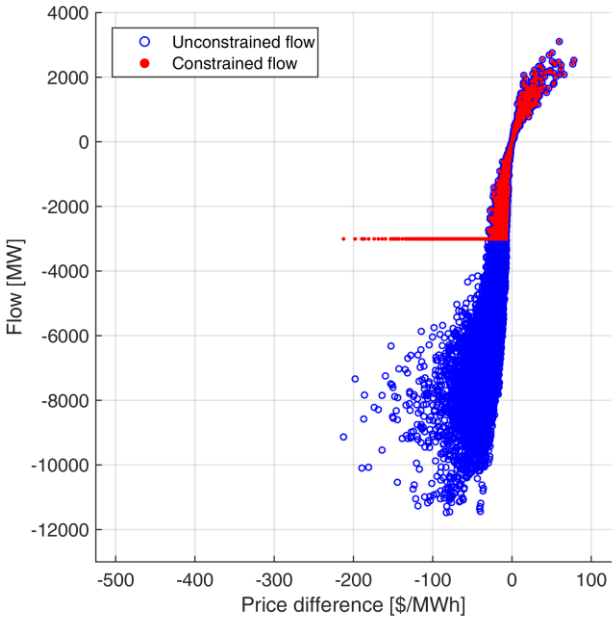

Figure 7. Flow sensitivity to the price difference (elastic load) year 2024.

Fig. 8 illustrates the path utilization duration curves. As expected, the magnitude of flow under the elastic demand case is greater than with the inelastic demand. The flow is truncated according to the path transfer capacity expansions.

The maximum annual surplus increase under the inelastic and the elastic demands are $703 M and $635 M, respectively. The annual surplus increase for the existing path transfer capacity under the inelastic and the elastic demands are $298 M and $156 M. The surplus increase, EUF and EPTDF are summarized in table II. The path capacity expansion increases both EUF and EPTDF. A cost-benefit analysis would be required to determine the optimal transfer capacity of the path.

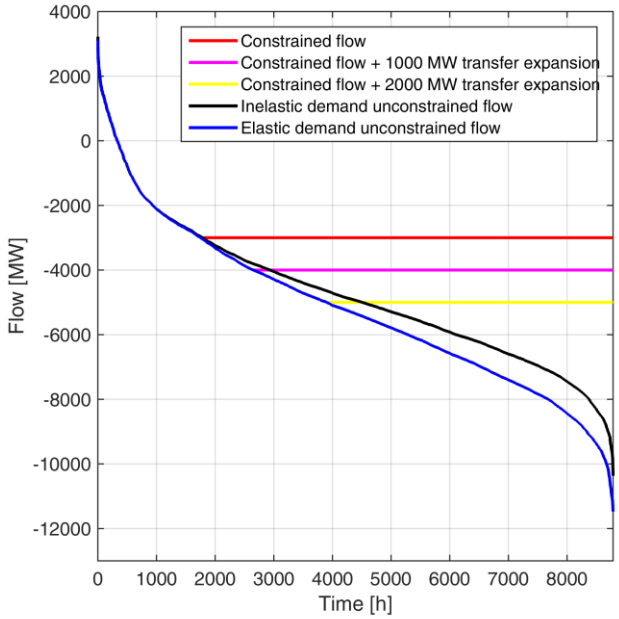

Figure 8. Path utilization duration curve for year 2024.

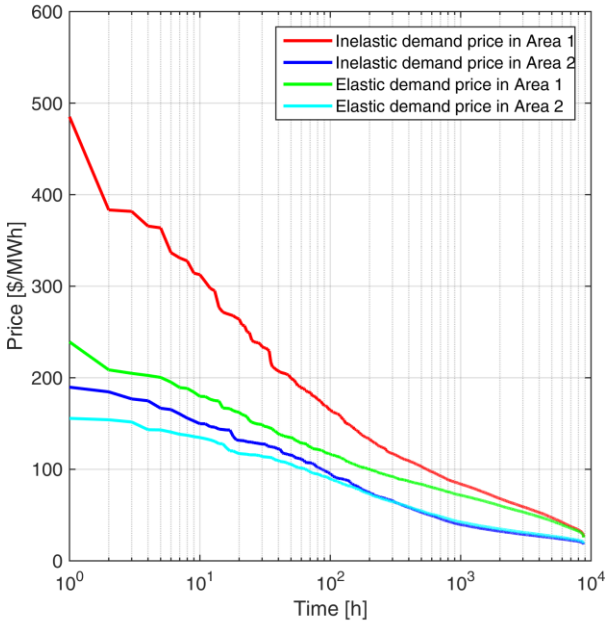

Figure 9. Price duration curve (stand-alone) year 2030.

TABLE II. RESULTS FOR YEAR 2024

Scenario	Inelastic Demand			Elastic Demand		
	Annual surplus increase [M$]	***EUF [%]***	***EPTDF [MW/($/MWh)]***	***Annual surplus increase [M$]***	***EUF [%]***	***EPTDF [MW/($/MWh)]***
Stand-alone	0	0	0	0	0	0
Existing transfer capacity	298	42	40	196	31	67
1000 MW transfer expansion	430	61	52	302	47	88
2000 MW transfer expansion	545	78	63	406	64	107
Copper-sheet	703	100	88	635	100	151

The same analysis is performed for the year 2030, assuming a case where wind capacity increases such that the annual generation from additional wind is equal to the demand growth (0.7% per year [11]). Figs. 9 and 10 show the price duration curves under inelastic and elastic demands. In comparison to the year 2024, the market clearing price is lower. The reason is wind, which is a zero-marginal cost resource, is a greater portion of the generation mixture, and influences the market price more significantly. This means that as wind penetration level increases, the producer surplus decreases, and maybe some supply units cannot recover their investment costs.

Fig. 11 illustrates the path utilization duration curves. In comparison with year 2024, the magnitude of the optimal flow is greater, because the demand and the wind generation are greater, and a greater flow is required to balance market prices.

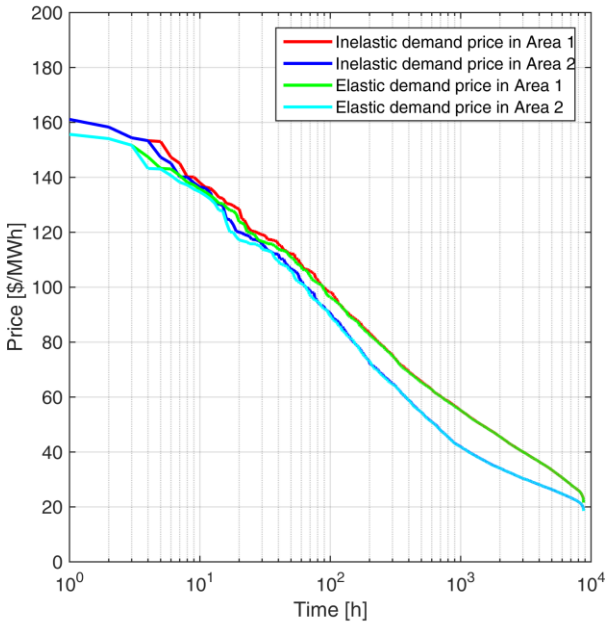

Figure 10. Price duration curve (with transfer constraint) year 2030.

Simulation results for 2030 are listed in table III. In comparison to 2024, the EUF is almost the same, but the EPTDF increases, because the flow is greater and the price difference is smaller in 2030 relatively.

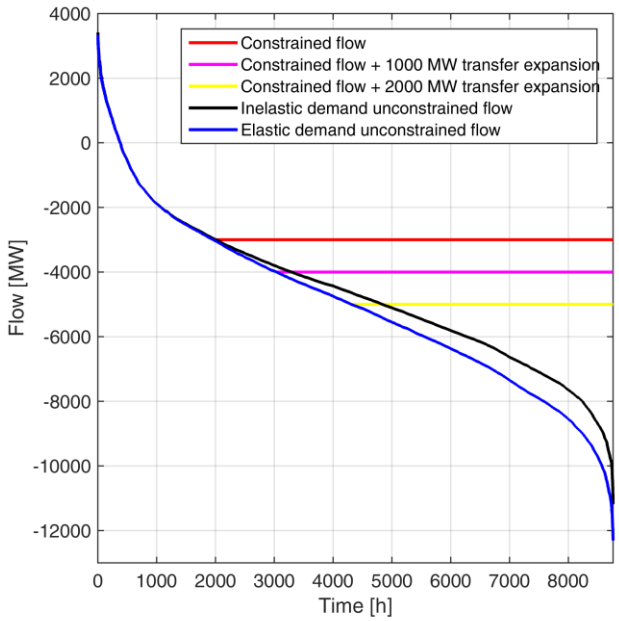

Figure 11. Path utilization duration curve for year 2030.

TABLE III. RESULTS FOR YEAR 2030

Scenario	Inelastic Demand			Elastic Demand		
	Annual surplus increase [M$]	*EUF [%]*	*EPTDF [MW/($/MWh)]*	*Annual surplus increase [M$]*	*EUF [%]*	*EPTDF [MW/($/MWh)]*
Stand-alone	0	0	0	0	0	0
Existing transfer capacity	232	42	54	160	32	84
1000 MW transfer expansion	333	60	69	243	48	109
2000 MW transfer expansion	419	76	83	323	64	132
Copper-sheet	549	100	106	502	100	185

IV. CONCLUSION

This paper assesses the impact of demand response integration and transmission capacity expansion on the electricity generation and inter-change scheduling. A surplus maximizing scheduling method is proposed and tested on a hypothetical system consisting of two consolidated areas that loosely represents the Western Interconnection. For given 2024 forecast data with hourly resolution, the stand-alone, copper-sheet (unconstrained-flow) and constrained-flow schedules are determined and compared. The additional annual surplus is $196 M under the elastic demand, for the existing path transfer capacity, which is only one-third of the maximum possible surplus increase. The path economic utilization factor and the economic power transfer distribution factor shows the sensitivity of the flow to the price difference is found 67 MW/($/MWh). The results for the year 2030, where additional wind electricity supplies the demand growth alone, show that a greater penetration of wind causes the path to be utilized relatively more. Future work is to develop a multi-area model for the WECC interconnection, and solve the constraint flow problem.

ACKNOWLEDGMENT

This work was supported by grants from Natural Resources Canada and the Pacific Institute of Climate Solutions. The Pacific Northwest National Laboratory is operated for the US Department of Energy by Battelle Memorial Institute under Contract DE-AC05-76RL08130.

REFERENCES

[1] Q. QDR. Benefits of demand response in electricity markets and recommendations for achieving them. US Dept. Energy, Washington, DC, USA, Tech. Rep. 2006.

[2] Q. Wang, C. Zhang, Y. Ding, G. Xydis, J. Wang, J. Østergaard. Review of real-time electricity markets for integrating distributed energy resources and demand response. Applied Energy, 138:695-706. 2015.

[3] C. L. Su, D. Kirschen. Quantifying the effect of demand response on electricity markets. IEEE Transactions on Power Systems, 24(3):1199-207. 2009.

[4] H. G. Kwag, J. O. Kim. Optimal combined scheduling of generation and demand response with demand resource constraints. Applied Energy, 96:161-70. 2012.

[5] H. Wu, M. Shahidehpour, A. Alabdulwahab, A. Abusorrah. Demand response exchange in the stochastic day-ahead scheduling with variable renewable generation. IEEE Transactions on Sustainable Energy, 6(2):516-25. 2015.

[6] P. Santoro, V. Galdi, V. Calderaro, G. Gross. Quantification of variable effects of demand response resources on power systems with integrated energy storage and renewable resources. In Power Tech, IEEE Eindhoven, pp. 1-6. 2015.

[7] S. Behboodi, D. P. Chassin, C. Crawford, and N. Djilali. Renewable resources portfolio optimization in the presence of demand response. Applied Energy, 162:139-48. 2016.

[8] G. Stern, J. H. Yan, P. B. Luh, W. E. Blankson. What objective function should be used for optimal auctions in the ISO/RTO electricity market?. In Power Engineering Society General Meeting, IEEE. 2006.

[9] S. Stoft. Power System Economics: Designing Markets for Electricity. Piscataway: Wiley-IEEE Press. 2002.

[10] T. B. Nguyen, N. Samaan, C. Jin. Evaluation of production cost savings from consolidation of balancing authorities in the US Western Interconnection under High wind and solar penetration. In Technologies for Sustainability (SusTech), IEEE Conference. pp. 9-14. 2014.

[11] A. E. MacDonald, C. T. Clack, A. Alexander, A. Dunbar, J. Wilczak, Y. Xie. Future cost-competitive electricity systems and their impact on US CO_2 emissions. Nature Climate Change. 2016.

[12] N. Samaan, M. Milligan, M. Hunsaker, T. Guo. Three-stage production cost modeling approach for evaluating the benefits of intra-hour scheduling between balancing authorities. In Power & Energy Society General Meeting, IEEE. pp. 1-5. 2015.

[13] S. Behboodi, D. P. Chassin, C. Crawford, and N. Djilali. Renewable resources portfolio optimization in the presence of demand response. Applied Energy, 162:139-48. 2016.

[14] D. P. Chassin, S. Behboodi, C. Crawford, and N. Djilali. Agent-Based Simulation for Interconnection-Scale Renewable Integration and Demand Response Studies. Engineering, 1(4):422-435. 2016. <http://engineering.org.cn/EN/10.15302/J-ENG-2015109#1>

[15] WECC System Adequacy Planning (SAP) Department. Release notes for WECC 2024 common case; April 2015. <http://tinyurl.com/mdch3ml>.